nrp **Nutrition Research and Practice**

Original Research

Check for updates

Skin protective effect of Indian gooseberry and barley sprout complex on skin dryness, wrinkles, and melanogenesis by cell models

Minhee Lee [iD] [1,2], **Dakyung Kim** [iD] [1], **Mi-Ryeong Park** [iD] [3], **Soyoung Kim** [iD] [3], **Jong-Lae Kim** [iD] [3], **Ok-Kyung Kim** [iD] [4§], and **Jeongmin Lee** [iD] [1,2§]

[1]Department of Medical Nutrition, Kyung Hee University, Yongin 17104, Korea
[2]Department of Food Innovation and Health, Kyung Hee University, Yongin 17104, Korea
[3]HLscience Co., Ltd, Uiwang 16004, Korea
[4]Division of Food and Nutrition and Human Ecology Research Institute, Chonnam National University, Gwangju 61186, Korea

OPEN ACCESS

§**Corresponding Authors:**

Ok-Kyung Kim
Division of Food and Nutrition and Human Ecology Research Institute, Chonnam National University, 77 Yongbong-ro, Buk-gu, Gwangju 61186, Korea.
Tel. +82-62-530-1334
Fax. +82-62-530-1339
Email. 20woskxm@jnu.ac.kr

Jeongmin Lee
Departments of Medical Nutrition and Food Innovation and Health, Kyung Hee University, 1732 Deogyeong-daero, Giheung-gu, Yongin 17104, Korea.
Tel. +82-31-201-3838
Email. jlee2007@khu.ac.kr

ORCID iDs
Minhee Lee [iD]
https://orcid.org/0000-0002-8820-4395

ABSTRACT

BACKGROUND/OBJECTIVES: UV radiation is a major factor contributing to DNA damage in skin cells, including stem cells and mesenchymal stem cells, leading to the depletion of these crucial cells. This study examined whether a mixture of Indian gooseberry and barley sprout (IB) could inhibit UVB irradiation and 3-isobutyl-1-methylxanthine (IBMX)-induced photoaging and oxidative stress in the skin using HaCaT, Hs27, and B16F10 cells.

MATERIALS/METHODS: The moisturizing-related factors, the collagen synthesis-related c-Jun N-terminal kinase (JNK)/c-Fos/c-Jun/matrix metalloproteinases (MMPs) pathway, and the melanogenesis-related cyclic adenosine monophosphate (cAMP)/protein kinase A (PKA)/cAMP-responsive binding protein (CREB)/melanocyte inducing transcription factor (MITF)/tyrosinase-related protein (TRP)/tyrosinase activation pathways were analyzed *in vitro* by an enzyme-linked immunosorbent assay, real-time polymerase chain reaction, and Western blot analysis.

RESULTS: The IB complex increased the hyaluronic acid and sphingomyelin levels and the collagenase inhibitory activity, enhanced hydration-related factors, including collagen, *hyaluronic acid synthase* (*HAS*), *elastin, long chain base subunit 1* (*LCB1*) (*serine palmitoyltransferase; SPT*), and *delta 4-desaturase sphingolipid 1* (*DEGS1*), modulated the inflammatory cytokines levels, antioxidant enzyme activities and the NF-κB/MMPs/cyclooxygenase-2 (COX-2) pathway in UVB-irradiated HaCaT cells, and inhibited wrinkle formation by down-regulation of the JNK/c-Fos/c-Jun/MMP pathway and up-regulation of the *transforming growth factor-β receptor I* (*TGFβR1*)/small mothers against decapentaplegic homolog (Smad3)/*procollagen type I* pathway in UVB-irradiated Hs27 cells. Moreover, the IB complex prevented melanin production by down-regulating the PKA/CREB/MITF/TRP-1/TRP-2 pathway in IBMX-induced B16F10 cells.

CONCLUSION: These findings suggest that the IB complex has the potential to serve as a safeguard, shielding the skin from UVB radiation-induced photo-damage.

Keywords: Skin; UV radiation; *Emblica officinalis*; *Hordeum vulgare*

Generated by Xmlinkpress

Dakyung Kim
https://orcid.org/0000-0001-9619-5081
Mi-Ryeong Park
https://orcid.org/0009-0007-3679-5393
Soyoung Kim
https://orcid.org/0009-0003-8964-6827
Jong-Lae Kim
https://orcid.org/0009-0008-0450-5539
Ok-Kyung Kim
https://orcid.org/0000-0002-8338-2571
Jeongmin Lee
https://orcid.org/0000-0002-3568-5906

INTRODUCTION

The skin is the largest organ of the body and serves as a crucial interface between the internal and external environments, protecting against pathogens, UV radiation, and harmful chemicals. Its intricate features are partly responsible for various physiological functions. The skin comprises the epidermis, dermis, and subcutaneous tissue. The epidermis, housing keratinocytes, safeguards the skin by minimizing heat and moisture loss. In addition, it features Merkel cells, Langerhans' cells, and melanocytes. The dermis exists beneath the epidermis and consists of fibroblasts and an extracellular matrix (ECM) with glycoproteins, proteoglycans, elastin, collagen, and hyaluronic acid [1,2].

Skin aging manifests in two forms: intrinsic and extrinsic aging, characterized by dyspigmentation, elasticity decline, wrinkles, and fragility. Intrinsic aging involves a thinned epidermis, cell loss, and skin wrinkling, whereas extrinsic aging, known as photoaging, results from accumulated damage caused by UV exposure [3,4]. Exposure to UV radiation in the epidermis induces reactive oxygen species (ROS) and reactive nitrogen species (RNS) that break down the antioxidant defense system, leading to oxidative stress. UVB-irradiated oxidative stress contributes to increased water loss, resulting in skin dryness. In addition, it stimulates the expression of matrix metalloproteinases (MMPs), leading to elastin degradation, and activates the enzyme tyrosinase, which is associated with melanin production. Moreover, it triggers protein degradation and pro-inflammatory cytokine production, culminating in the formation of skin wrinkles [5-7].

Indian gooseberry (*Emblica officinalis*), also called amla, has been investigated to understand its potential health benefits and functional properties, such as gastroprotective, antioxidant, anti-obesity, anti-cancer, anti-diabetic, and immunomodulatory effects. In addition, it has also been studied for its anti-bacterial, anti-fungal, and other medicinal properties [8-11]. Barley sprouts (*Hordeum vulgare* L.) have been reported to enhance the phenolic bioactive-linked anti-glycemic, anti-obesity, anti-inflammatory, and anti-cardiovascular effects [12-14]. The consumption of Indian gooseberry or barley sprouts has been popularized in the form of pharmaceuticals, cosmetic products, and health foods, but insufficient research on the combined health benefits and mechanism of mixtures of Indian gooseberry and barley sprout (IB) has been conducted. The authors previously investigated the anti-obesity effects of an IB complex using 3T3-L1 cells and high-fat diet-fed animal models [15,16]. The current experiments investigated the mechanisms underlying the effects of IB complex on UVB-induced skin oxidative stress by analyzing the hyaluronic acid and ceramide synthesis factors, c-Jun N-terminal kinase (JNK)/c-Fos/c-Jun/MMPs and *transforming growth factor-β receptor I* (*TGF-βRI*)/small mothers against decapentaplegic homolog (Smad) pathways, and the cyclic adenosine monophosphate (cAMP)/protein kinase A (PKA)/cAMP-responsive binding protein (CREB)/melanocyte inducing transcription factor (MITF)/tyrosinase-related protein (TRP)/tyrosinase activation pathways.

MATERIALS AND METHODS

IB complex preparation
Indian gooseberry extract powder (I) and barley sprout juice powder (B) were provided by HL Science Co., Ltd. (Uiwang, Korea), and the IB complex was composed of I:B = 2:1 (w/w). The extraction methods of I and B are detailed elsewhere [16]. The powders were stored at −20°C until the experiments were conducted.

Cell culture and treatments

The HaCaT (human keratinocytes) cells were provided by Professor Hwang of the College of Life Sciences, Kyung Hee University. Hs27 (human fibroblasts), and the B16F10 (melanoma) cells were purchased from the American Type Culture Collection (ATCC). Each cell line was cultured in Dulbecco's modified Eagle's medium (DMEM) supplemented with 10% fetal bovine serum (FBS), 1% penicillin/streptomycin, 1% L-glutamine, and 1% sodium pyruvate. Each cell line seeded for each experiment was washed. The HaCaT and Hs27 cells were exposed to 50 mJ/cm^2 of UV rays using five Sankyo Denki G5T5 lamps (Sankyo Denki Co., Yokohama, Japan). The B16F10 cells were differentiated by treating them with 3-isobutyl-1-methylxanthine (IBMX) (250 μM) for 72 h to induce melanin synthesis. All cells stimulated with UVB or IBMX were treated with ascorbic acid (100 μg/mL) or arbutin (100 μg/mL) and the IB complex (50, 100, and 200 μg/mL; the cell viability of HaCaT, Hs27, and B16F10 cells was not affected by the IB complex at those concentrations, data not shown).

Measurement of hyaluronic acid, sphingomyelin, collagenase inhibitory activity, elastase inhibitory activity, pro-inflammatory cytokines, and antioxidant enzyme activity levels

HaCaT cells were lysed, and hyaluronic acid, sphingomyelin, pro-inflammatory cytokines (tumor necrosis factor [TNF]-α, interleukin [IL]-1β, and IL-6), and the antioxidant enzyme activity (superoxide dismutase [SOD], catalase [CAT], and glutathione peroxidase [GPx]) levels were then determined using a Hyaluronic acid ELISA Kit (BioVision Inc., Milpitas, CA, USA), Sphingomyelin Assay Kit (Abcam, Cambridge, UK), TNF-α, IL-1β, and IL-6 DuoSet ELISA kits (all from R&D System, Minneapolis, MN, USA), and SOD, CAT, and GPx activity kits (all from BioVision Inc.), respectively, according to the manufacturer protocols.

Measurement of the collagenase inhibitory activity and elastase inhibitory activity levels

The collagenase and elastase inhibitory activities were assayed using the methods reported by Wünsch and Heidrich [17] and Cannell *et al.* [18], respectively.

Measurement of intracellular melanin and glutathione (GSH) contents

The B16F10 cells were lysed, and the GSH levels were determined using a Glutathione Assay Kit (BioVision Inc.) according to the manufacturer's protocols.

Measurement of tyrosinase activity, nitric oxide, and cAMP Levels

The B16F10 cells were lysed, and the tyrosinase activity and the nitric oxide (NO) and cAMP levels were then determined using a Tyrosinase Activity Assay Kit (Abcam), Nitric Oxide Assay Kit (Abcam), and cAMP ELISA Kit (Enzo Life Sciences, Plymouth Meeting, PA, USA), respectively, according to the manufacturer protocols.

Isolation of total RNA and reverse transcription-PCR

The total RNA from cells was isolated using a RNeasy Mini kit (Qiagen, Valencia, CA, USA). Complementary DNA synthesis was performed using an iScript™ cDNA Synthesis Kit (Bio-Rad Laboratories, Hercules, CA, USA). PCR amplification consisted of 40 cycles of 95°C for 15 s, 58°C for 15 s, and 72°C for 30 s with a SYBR Green PCR Master Mix (Bio-Rad Laboratories) and primer pairs (**Table 1**). The data were analyzed using CFX Maestro™ Analysis Software (Bio-Rad Laboratories).

Table 1. Primer sets used for real-time polymerase chain reaction

Gene	Sequence
COL1A1 (Human)	F 5'-GCC TCG GAG GAA ACT TTG C-3'
	R 5'-TCC GGT TGA TTT CTC ATC ATA GC-3'
COL1A2 (Human)	F 5'-GCT ACC CAA CTT GCC TTC ATG-3'
	R 5'-GCA GTG GTA GGT GAT GTT CTG AGA-3'
COL3A1 (Human)	F 5'-GGG AAT GGA GCA AAA CAG TCT T-3'
	R 5'-CAT AGG GTG CAA TAT CTA CAA TAG GTA GTC-3'
COL4A1 (Human)	F 5'-CGT AAC TAA CAC ACC CTG CTT CAT-3'
	R 5'-CAC TAT TGA AAG CTT ATC GCT GTC TT-3'
HAS1 (Human)	F 5'-TCA GGG AGT GGG ATT GTA GGA-3'
	R 5'-AGG CCT AGA GGA CCG CTG AT-3
HAS2 (Human)	F 5'-GAA ACA GCC CCA GCC AAA-3'
	R 5'-AAG ACT CAG CAG AAC CCA GGA A-3'
HAS3 (Human)	F 5'-TGC TTG CCC TCC AAA TGT C-3'
	R 5'-CCT CTT GTC TGC TGT CCA CCT T-3'
Elastin (Human)	F 5'-GTC GGA GTC GGA GGT ATC-3'
	R 5'-TGA GAA GAG CAA ACT GGG-3'
LCB1(SPT) (Human)	F 5'-CCA TGG AGT GGC CTG AAA GA-3'
	R 5'-CTG ACA CCA TTT GGT AAC AAT CCT A-3'
DEGS1 (Human)	F 5'-GCT GAT GGC GTC GAT GTA GA-3'
	R 5'-TGA AAG CGG TAC AGA AGA ACC A-3'
TGF-β RI (Human)	F 5'-TCC CGG CAG ATC AAC GA-3'
	R 5'-ACG CGG TCA CAA ACA TGG T-3'
PCOLCE (Human)	F 5'-TCT CCT CCG AAG GGA ATG AAC-3'
	R 5'-CAG CGG TGA CAC TGA GAT CTG-3'
Pro-COL1 (Human)	F 5'-GCC TCG GAG GAA ACT TTG C-3'
	R 5'-TCC GGT TGA TTT CTC ATC ATA GC-3'
GAPDH (Human)	F 5'-CCC CAC ACA CAT GCA CTT ACC-3'
	R 5'-TTG CCA AGT TGC CTG TCC TT-3'

HAS, *hyaluronic acid synthase*; *LCB1* (*SPT*), *long chain base subunit 1* (*serine palmitoyltransferase*); *DEGS1*, *dihydroceramide desaturase*; *TGF-β RI*; *transforming growth factor beta receptor 1, PCOLCE*; *procollagen C-endopeptidase enhancer*, *Pro-COL1*; *procollagen type I*; *GAPDH, glyceraldehyde-3-phosphate dehydrogenase*.

Protein extraction and Western blot analysis

The cells were lysed using a CelLytic™ MT cell lysis reagent (Sigma, St. Louis, MO, USA). The protein samples (100 µg) were separated using a 10% Mini-PROTEAN® TGX™ Precast Protein Gel (Bio-Rad Laboratories) and electrotransferred onto polyvinylidene difluoride (PVDF) membranes (Bio-Rad Laboratories). The membranes were blocked with 5% skimmed milk in Tris-buffered saline with 0.1% Tween 20 (TBST) for 1 h, and incubated for 12 h at 4°C with antibodies against CerS4 (LASS4), p-IκB, IκB, p65, p-p65, COX2, JNK, p-JNK, c-Fos, p-c-Fos, c-Jun, p-c-Jun, MMP-1, MMP-2, MMP-3, MMP-9, Smad3, p-Smad3, PKA, p-PKA, CREB, p-CREB, MITF, TRP-1, TRP-2, and β-actin (1:1,000). The antibodies were purchased from Cell Signaling (Beverly, MA, USA), Abcam, and LSbio (Seattle, WA, USA). After incubation with the primary antibody, the membranes were incubated with a secondary antibody (anti-rabbit IgG HRP-linked antibody, 1:5,000; Cell Signaling) for 1 h at room temperature. The protein bands were detected with EzWestLumi Plus (ATTO, Tokyo, Japan), developed using Ez-Capture II (ATTO), and quantified using CS Analyzer 3.0 (ATTO).

Statistical analysis

All results are reported as the mean ± SD. The data were assessed statistically using Duncan's multiple range tests after one-way analysis of variance (ANOVA) using SPSS PASW Statistic v.23.0 (SPSS Inc., Chicago, IL, USA). The differences were considered statistically significant at $P < 0.05$.

RESULTS

Effects of IB complex on hyaluronic acid, sphingomyelin in UVB-irradiated HaCaT cells, and collagenase inhibitory activity, and elastase inhibitory activity

The effects of the IB complex on hyaluronic acid and sphingomyelin in UVB-irradiated HaCaT cells were analyzed using ELISA methods. The levels of hyaluronic acid were significantly lower in the control group than in the normal control (NC) group, but substantial improvements were observed after the L-ascorbic acid (AA), IB complex 100, and IB complex 200 treatments, showing 44.6%, 17.9%, and 31.7% enhancements, respectively ($P < 0.05$) (**Fig. 1A**). The sphingomyelin levels were significantly lower in the control group than the NC group ($P < 0.05$). The UVB-irradiated HaCaT cells treated with AA, IB complex 100, and IB complex 200 showed significantly higher sphingomyelin levels than the control group (72.7%, 25.0%, and 50.5%, respectively; $P < 0.05$) (**Fig. 1B**).

The effects of the IB complex on the collagenase and elastase inhibitory activities were analyzed using the methods reported by Wünsch and Heidrich [17] and Cannell *et al*. [18]. The collagenase and elastase inhibitory activities were markedly higher in the AA group than in the IB group (55.5% and 47.4%). Furthermore, the IB complexes induced dose-dependent increases in the collagenase and elastase inhibitory activities. The collagenase inhibitory activities in the IB complex 50, IB complex 100, and IB complex 200 were 6.6%, 18.8%, and 39.8%, respectively. The elastase inhibitory activities in the IB complex 50, IB complex 100, and IB complex 200 were 7.1%, 15.0%, and 31.6%, respectively ($P < 0.05$) (**Fig. 2A and B**).

Effects of IB complex on mRNA expression of the factors related to collagen synthesis and skin moisturizing in UVB-irradiated HaCaT cells

The UVB-irradiated HaCaT cells were analyzed using real-time PCR to investigate the collagen synthesis and skin moisturizing-related factors affected by the IB complex. In the control group, the mRNA expressions of *COL1A1*, *COL1A2*, *COL3A1*, *COL4A1*, *hyaluronic acid synthase* (*HAS*) *1*, *HAS2*, *HAS3*, *elastin*, *long chain base subunit 1* (*LCB1*) (*serine palmitoyltransferase*; *SPT*), and *delta 4-desaturase sphingolipid 1* (*DEGS1*) were significantly lower than the NC group. In particular, the AA group showed significant increases in these expressions ($P < 0.05$) (**Fig. 3**). The mRNA
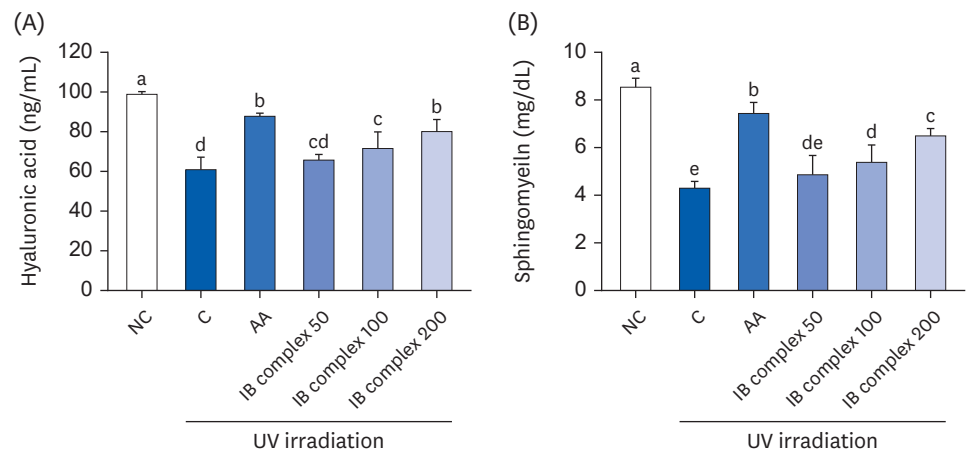

Fig. 1. Effects of the IB complex on hyaluronic acid (A) and Sphingomyelin (B) in UVB-irradiated HaCaT cells. The cells were treated with UVB (50 mJ/cm²) except NC and incubated for 24 h with 100 μg/mL of AA and various concentrations (50, 100, and 200 μg/mL) of the IB complex. The values are presented as means ± SD.
IB, Indian gooseberry and barley sprout; NC, normal control; C, control; AA, L-ascorbic acid.
Different letters show a significant difference at $P < 0.05$, as determined by Duncan's multiple range test.
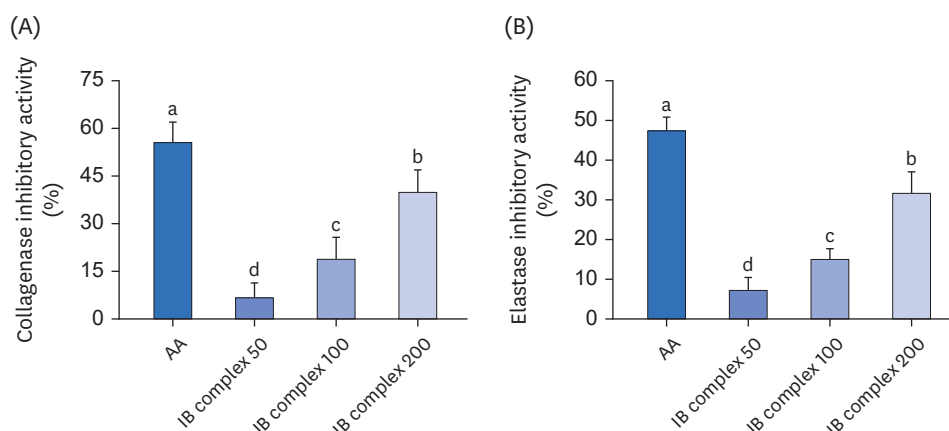
Fig. 2. Effects of the IB complex on the collagenase inhibitory activity (A) and elastase inhibitory activity (B). A 100 µg/mL of AA and various concentrations (50, 100, and 200 µg/mL) of the IB complex. The values are presented as the means ± SD.
IB, Indian gooseberry and barley sprout; AA, L-ascorbic acid.
Different letters show a significant difference at $P < 0.05$, as determined by Duncan's multiple range test.

expression levels of *COL1A1*, *COL1A2*, *COL3A1*, and *COL4A1* were higher in the IB complex 100 and IB complex 200 groups than in the control group (81.0% and 150.7%, 52.5% and 76.8%, 54.3% and 128.4%, and 87.3% and 148.2%, respectively; $P < 0.05$) (**Fig. 3A-D**). In addition, the mRNA expression levels of *HAS1*, *HAS2*, and *HAS3* were significantly higher in the IB complex 100 and IB complex 200 than in the control group (128.5% and 174.8%, 105.7% and 144.0%, and 135.4% and 159.6%, respectively; $P < 0.05$) (**Fig. 3E-G**). The mRNA expression of *elastin* was improved markedly in the IB complex-treated groups than in the control group (39.7–194.1%, $P < 0.05$) (**Fig. 3H**). Moreover, *LCB1* (*SPT*) and *DEGS1* expression levels were significantly higher in the IB complex 100 and IB complex 200 groups (72.2% and 144.5%, 71.8% and 94.5%, respectively) than in the control group ($P < 0.05$) (**Fig. 3I and J**). Therefore, the IB complex directly activated collagen synthesis and moisturizing factors in keratinocytes.

Effects of IB complex on inflammatory cytokines (TNF-α, IL-1β, IL-6), antioxidant activities (SOD, CAT, GPx), and protein expression of skin moisturizing-related factors in UVB-irradiated HaCaT cells

The effects of the IB complex on the inflammatory cytokines levels and antioxidant activities in UVB-irradiated HaCaT cells were examined using an ELISA kit. The levels of TNF-α, IL-1β, and IL-6 showed a significant increase in the control group compared to the NC group, while the AA group showed a significant decrease compared to the control group ($P < 0.05$) (**Fig. 4A-C**). The IB complex 100 showed significantly lower TNF-α and IL-6 levels than the control (20.8% and 23.4%, respectively; $P < 0.05$) (**Fig. 4A-C**). Moreover, the IB complex 200 group showed a significant decrease in the TNF-α, IL-1β, and IL-6 levels compared to the control group (35.9%, 31.8%, and 36.0%, respectively; $P < 0.05$) (**Fig. 4A-C**). The activities of the antioxidant enzymes (SOD, CAT, and GPx) were significantly lower in the control group than in the NC group. In contrast, the AA group showed significant improvement compared to the control group ($P < 0.05$) (**Fig. 4D-F**). Furthermore, the IB complex 100 showed significantly higher SOD and GPx activities than the control (78.4% and 88.1%, respectively; $P < 0.05$) (**Fig. 4D-F**), and the IB complex 200 showed remarkably higher SOD, CAT, and GPx activities than the control (118.9%, 58.4%, and 200.8%, respectively; $P < 0.05$) (**Fig. 4D-F**).
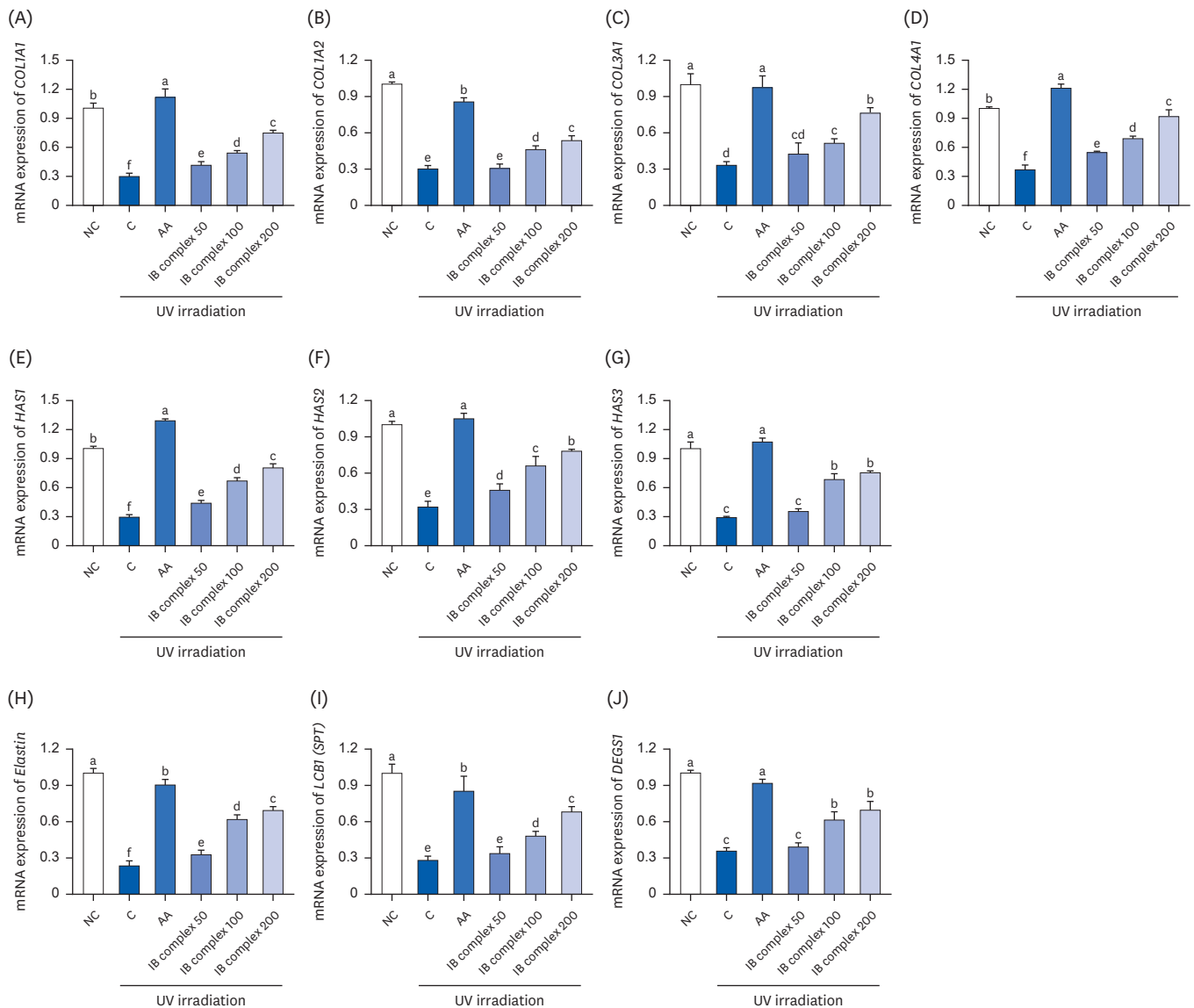
Fig. 3. Effects of the IB complex on *COL1A1* (A), *COL1A2* (B), *COL3A1* (C), *COL4A1* (D), *HAS1* (E), *HAS2* (F), *HAS3* (G), *Elastin* (H), *LCB1* (I), and *DEGS1* (J) in UVB-irradiated HaCaT cells. The cells were treated with UVB (50 mJ/cm²) except NC and incubated for 24 h with 100 µg/mL of AA and various concentrations (50, 100, and 200 µg/mL) of the IB complex. The values are presented as means ± SD.
IB, Indian gooseberry and barley sprout; *HAS*, hyaluronic acid synthase; *LCB1* (*SPT*), long chain base subunit 1 (*serine palmitoyltransferase*); *DEGS1*, desaturase sphingolipid 1; NC, normal control; C, control; AA, L-ascorbic acid.
The different letters show a significant difference at *P* < 0.05, as determined by Duncan's multiple range test.

The effects of the IB complex on the protein expression of skin moisturizing-related factors in UVB-irradiated HaCaT cells were examined using Western blot analysis. The protein expression of CerS4 was significantly lower in the control group than in the NC group; however, the protein expressions of p-IκB/IκB, p-p65/p65, MMP-1, MMP-2, MMP-9, and cyclooxygenase-2 (COX-2) were significantly higher in the control group than in the NC group (*P* < 0.05) (**Fig. 4G-N**). By contrast, the AA group exhibited a significant increase in the protein expression of Cers4 and a decrease in the protein expression of p-IκB/IκB, p-p65/p65, MMP-1, MMP-2, MMP-9, and COX-2 compared to the control group (*P* < 0.05) (**Fig. 4G-N**). The protein expression of CerS4 was significantly higher in the IB complex 100 and IB complex 200 than in the control group (14.0% and 30.9%, respectively; *P* < 0.05) (**Fig. 4G**). The cells treated
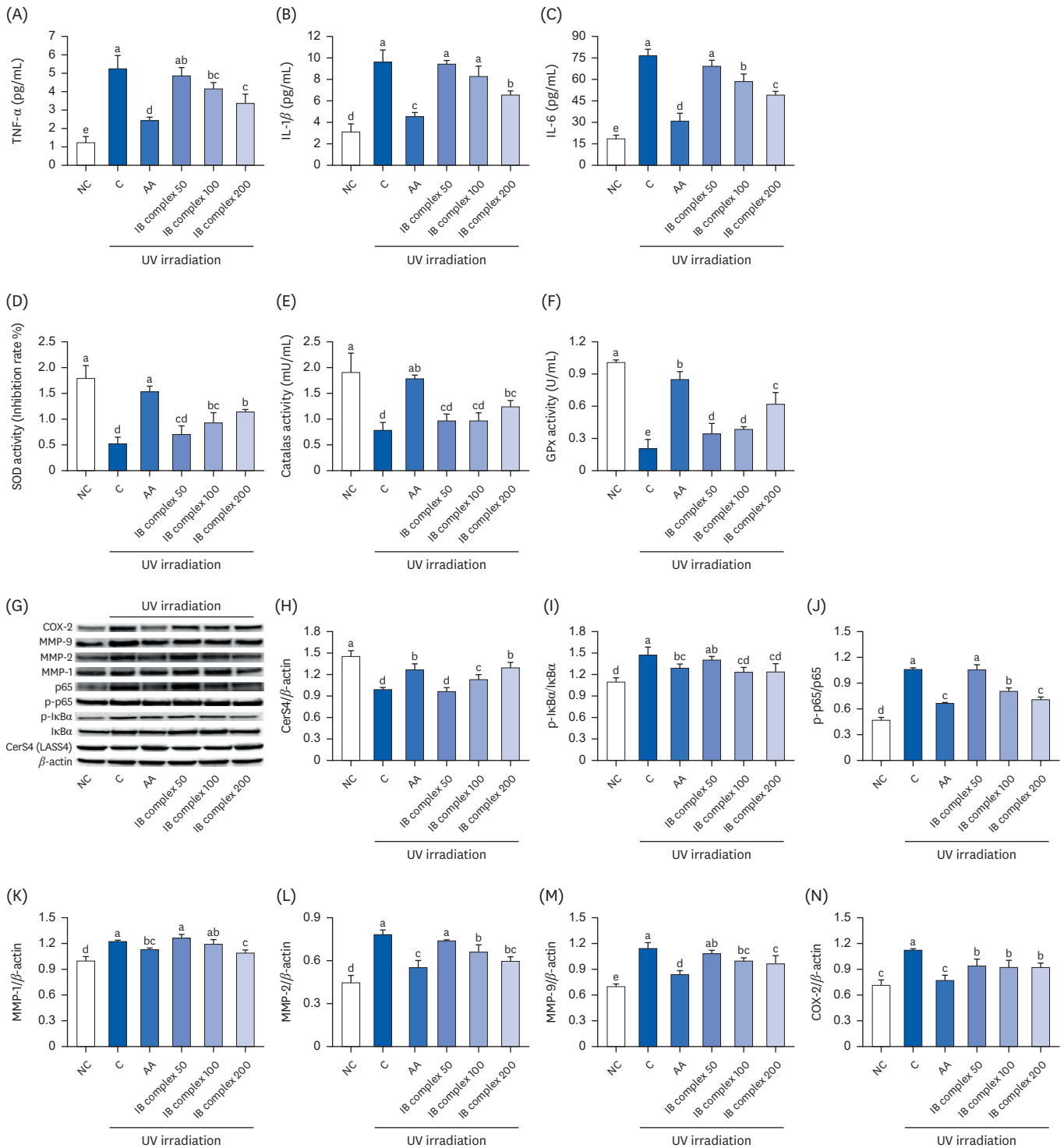
Fig. 4. Effects of the IB complex on TNF-α (A), IL-1β (B), IL-6 (C), SOD activity (D), CAT activity (E), GPx activity (F), western blot band (G), CerS4 (H), p-IκBα (I), p-p65 (J), MMP-1 (K), MMP-2 (L), MMP-9 (M), and COX-2 (N) in UVB-irradiated HaCaT cells. The cells were treated with UVB (50 mJ/cm²) except NC and incubated for 24 h with 100 μg/mL of AA and various concentrations (50, 100, and 200 μg/mL) of IB complex. The values are presented as means ± SD.
IB, Indian gooseberry and barley sprout; TNF, tumor necrosis factor; IL, interleukin; SOD, superoxide dismutase; CAT, catalase; GPx, glutathione peroxidase; MMP, matrix metalloproteinase; COX-2, cyclooxygenase-2; NC, normal control; C, control; AA, L-ascorbic acid.
Different letters show a significant difference at P < 0.05, as determined by Duncan's multiple range test.

with IB complex 100 and IB complex 200 exhibited a significant decrease in the protein expression of p-IκB/IκB, p-p65/p65, MMP-2, MMP-9, and COX-2 compared to the control group (16.1% and 15.8%, 24.2% and 33.2%, 15.5% and 23.7%, 12.7% and 15.4%, and 18.0% and 17.8%, respectively; $P < 0.05$) (**Fig. 4I, J, L-N**). MMP-1 protein expression was significantly lower in the IB complex 200 than in the control group (11.0%) ($P < 0.05$) (**Fig. 4K**). These findings suggest that the IB complex effectively adjusted the inflammatory cytokines, antioxidant enzyme activities, and protein expression of skin moisturizing-related factors in response to UVB irradiation.

Effects of the IB complex on the skin wrinkle-related factors in UVB-irradiated Hs27 cells

The skin wrinkle-related factors affected by the IB complex in the UVB-irradiated Hs27 cells were analyzed using real-time PCR and Western blot analysis. The mRNA expression of *TGF-β RI*, *procollagen C-endopeptidase enhancer* (*PCOLCE*), and *pro-COL1* was significantly lower in the control group than the NC group but higher in the AA group ($P < 0.05$) (**Fig. 5A-C**). The UVB-irradiated Hs27 cells treated with IB complex 100 and IB complex 200 showed a significant increase in the mRNA expression of *TGF-β RI* and *PCOLCE* compared to the control group (107.8% and 140.9%, 114.9% and 184.7%, respectively; $P < 0.05$) (**Fig. 5A and B**). In particular, the mRNA expression of *pro-COL1* showed a significant increase in the IB complex-treated group than the control group (32.0–153.2%, $P < 0.05$) (**Fig. 5C**). Moreover, the protein expression of p-JNK/JNK, p-c-Fos/c-Fos, p-c-Jun/c-Jun, MMP-1, MMP-3, and MMP-9 showed a significant increase in the control group than the NC group ($P < 0.05$). The UVB-irradiated Hs27 cells treated with AA showed a significant decrease in the protein expression of p-JNK/JNK, p-c-Fos/c-Fos, p-c-Jun/c-Jun, MMP-1, MMP-3, and MMP-9 ($P < 0.05$) On the other hand, Smad3 phosphorylation showed a significant decrease in the control groups compared to the NC group ($P < 0.05$). The UVB-irradiated Hs27 cells treated with AA showed a significant increase in Smad3 phosphorylation ($P < 0.05$) (**Fig. 5D-K**). The protein expression levels of p-JNK/JNK, p-c-Jun/c-Jun, MMP-1, MMP-3, and MMP-9 were substantially lower in the IB complex treated groups than in the control group (15.1–37.6%, 31.5–54.3%, 27.4–46.0%, 39.2–60.0%, and 18.8–47.9%, respectively; $P < 0.05$) (**Fig. 5D, E, G-J**). The protein expression of p-c-Fos/c-Fos was significantly lower in the IB complex 200 group than in the control groups (56.2%) ($P < 0.05$) (**Fig. 5F**). In addition, the UVB-irradiated Hs27 cells treated with IB complex showed a significant increase in Smad3 phosphorylation than the control group (55.3–200.9%) ($P < 0.05$) (**Fig. 5K**). Therefore, the IB complex directly controls the wrinkle-related factors in response to UVB irradiation.

Effects of the IB complex on the melanogenesis-related factors in IBMX-treated B16F10 cells

IBMX-treated B16F10 cells were analyzed using an ELISA kit and Western blot analysis to investigate the effects of the IB complex on the following: melanin content; tyrosinase activity, NO, cAMP, and GSH levels; and melanogenesis-related factors. The melanin content, tyrosinase activity, NO, and cAMP levels were significantly higher in the control group than the other groups, but the arbutin treatment applied to the IBMX-treated B16F10 cells induced a significant decrease in those levels compared to the control group ($P < 0.05$) (**Fig. 6A-D, F**). The glutathione levels were significantly lower in the control group than in the NC group, but the arbutin treatment of the IBMX-treated B16F10 cells induced a significant increase in those levels compared to the control group ($P < 0.05$) (**Fig. 6E**). The addition of the IB complex to IBMX-treated B16F10 cells with IB complex induced a dose-dependent decrease in the melanin contents compared to the control group (15.6–41.4%; $P < 0.05$) (**Fig. 6A and B**). The tyrosinase
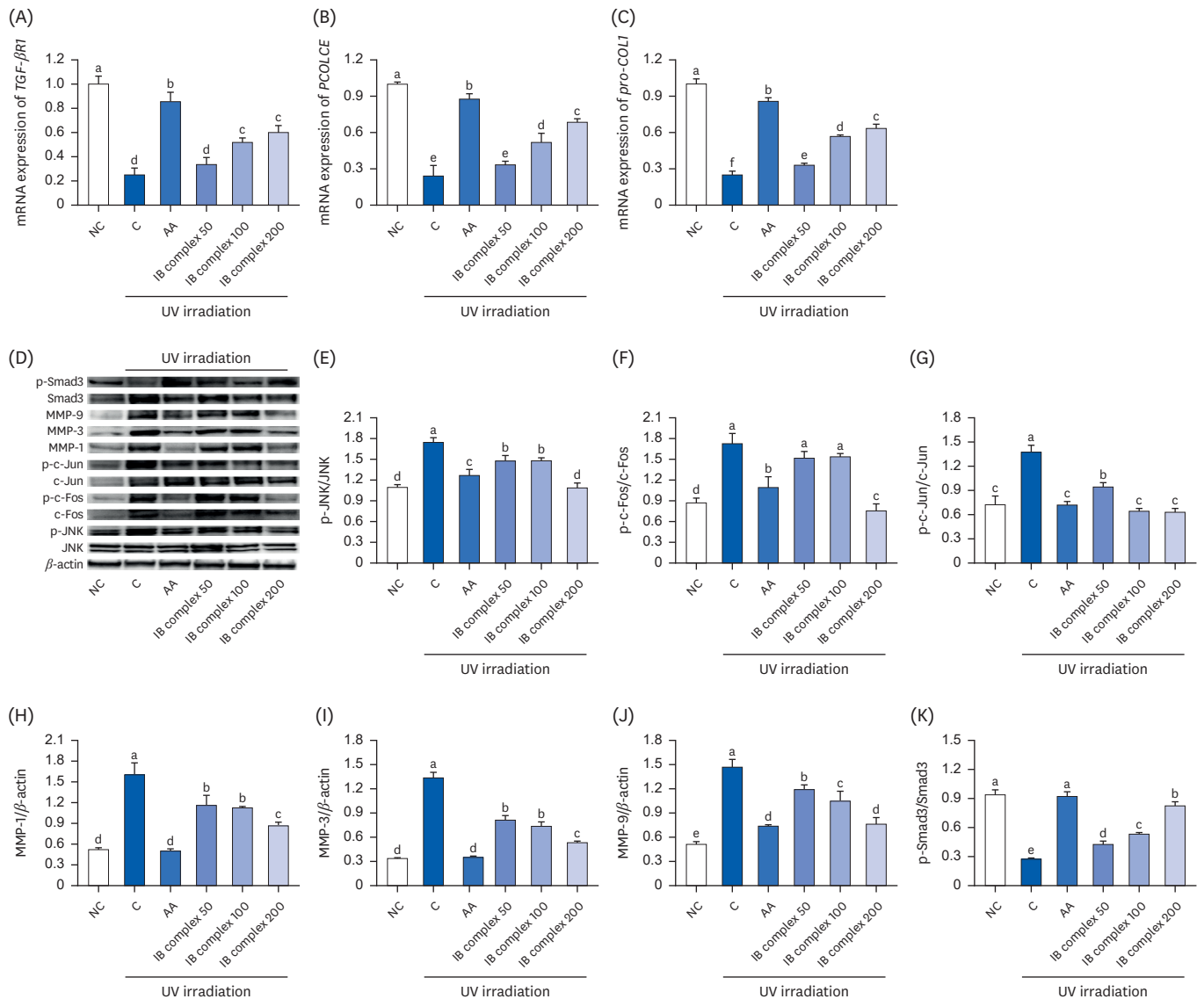
Fig. 5. Effects of the IB complex on *TGF-βR1* (A), *PCOLCE* (B), *Pro-COL1* (C), western blot band (D), p-JNK (E), p-c-FOS (F), p-c-Jun (G), MMP-1 (H), MMP-3 (I), MMP-9 (J), and p-Smad3 (K), in UVB-irradiated Hs27 cells. The cells were treated with UVB (50 mJ/cm²) except NC and incubated for 24 h with 100 µg/mL of AA and various concentrations (50, 100, and 200 µg/mL) of the IB complex. The values are presented as means ± SD.
IB, Indian gooseberry and barley sprout; *TGF-β RI, transforming growth factor-β receptor I*; *PCOLCE*, *procollagen C-endopeptidase enhancer*; *Pro-COL1*; *procollagen type I*; MMP, matrix metalloproteinase; Smad, small mothers against decapentaplegic homolog; NC, normal control; C, control; AA, L-ascorbic acid. Different letters show a significant difference at *P* < 0.05, as determined by a Duncan's multiple range test.

activities were significantly lower in the IB complex 100 and IB complex 200 than in the control group (15.0% and 32.4%, respectively; *P* < 0.05) (**Fig. 6C**). The NO levels were decreased significantly by the addition of the IB complex to the IBMX-treated B16F10 cells compared to the control group (13.0–31.3%; *P* < 0.05) (**Fig. 6D**). The addition of the IB complex to the IBMX-treated B16F10 cells showed a dose-dependent increase in the glutathione levels than the control group (72.0–240.3%; *P* < 0.05) (**Fig. 6E**), and the cAMP levels were significantly lower in the IB complex 200 group than in the control group (17.5%) (*P* < 0.05) (**Fig. 6F**). The protein expressions of p-PKA/PKA, p-CREB/CREB, MITF, TRP-1, and TRP-2 were significantly higher in the control group than in the NC group, but the arbutin treatment of IBMX-treated B16F10 cells induced a significant decrease in p-PKA/PKA, p-CREB/CREB, MITF, TRP-1, and TRP-2 than in
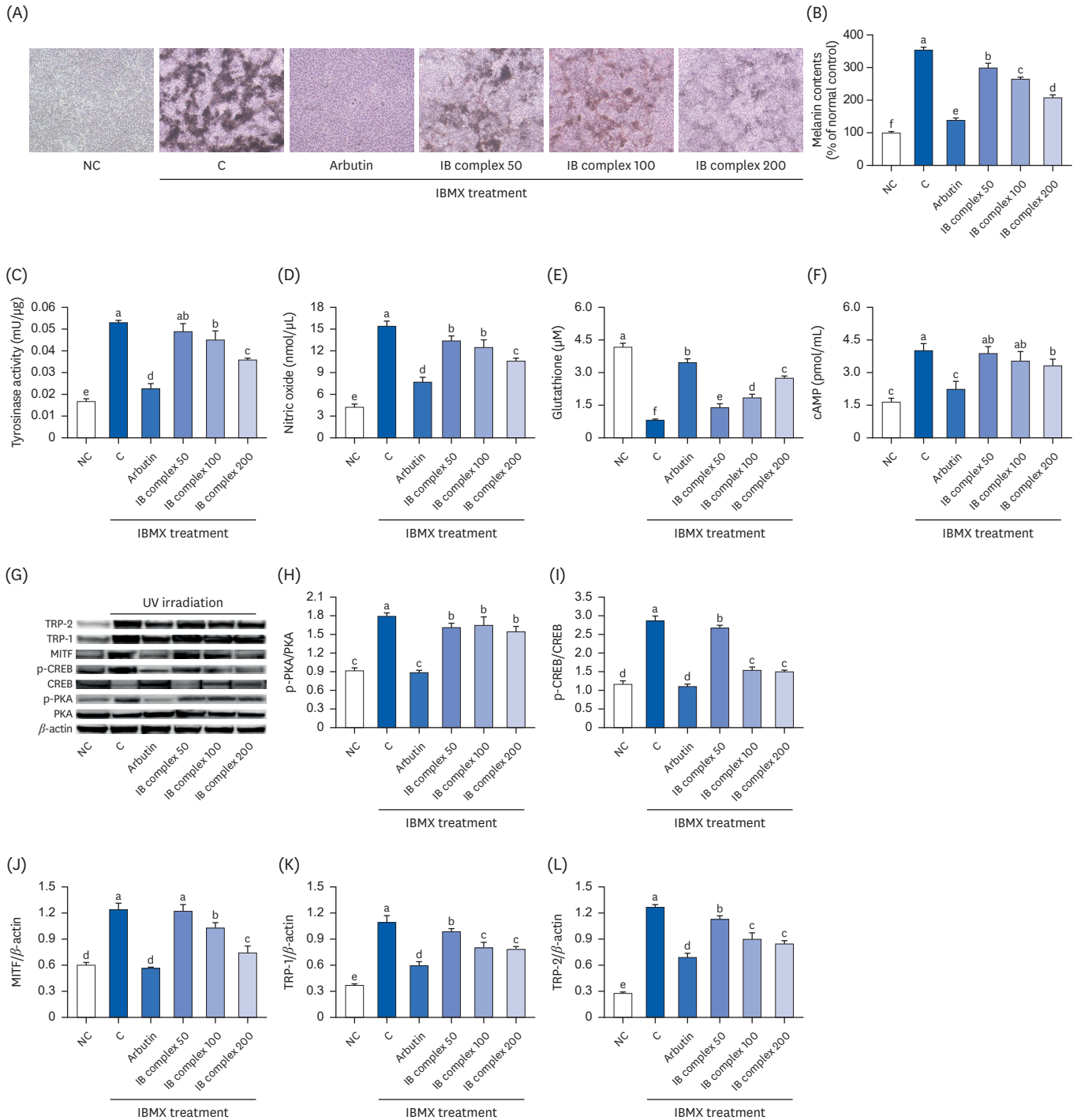
Fig. 6. Effects of the IB complex on the skin melanogenesis-related factors, melanin contents (A, B), tyrosinase activity (C), NO (D), Glutathione (E), cAMP (F), western blot band (G), p-PKA (H), p-CREB (I), MITF (J), TRP-1 (K), and TRP-2 (L) in IBMX-irradiated B16F10 cells. The cells were treated with 250 μM IBMX except for NC and incubated for 24 h with 100 μg/mL of arbutin and various concentrations (50, 100, and 200 μg/mL) of the IB complex. The values are presented as the means ± SD.

IB, Indian gooseberry and barley sprout; NO, nitric oxide; cAMP, cyclic adenosine monophosphate; PKA, protein kinase A; CREB, cAMP-responsive binding protein; MITF, melanocyte inducing transcription factor; TRP, tyrosinase-related protein; IBMX, 3-isobutyl-1-methylxanthine; NC, normal control; C, control. Different letters show a significant difference at $P < 0.05$ as determined by a Duncan's multiple range test.

the control group ($P < 0.05$) (**Fig. 6G-L**). The protein expression of p-PKA/PKA, p-CREB/CREB, TRP-1, and TRP-2 in the IBMX-treated B16F10 cells exhibited a marked decrease in IB complex treatment groups than the control group (8.2–14.0%, 6.7–47.6%, 9.7–28.5%, and 10.8–33.3%, respectively; $P < 0.05$) (**Fig. 6G-I, K, L**), and the protein expression of MITF was significantly decreased in the IB complex 100 and IB complex 200 groups than the control group (17.2% and 40.1%, respectively; $P < 0.05$) (**Fig. 6J**). These results suggested that the IB complex directly inhibited melanogenesis in IBMX-treated melanocytes.

DISCUSSION

Skin aging is caused by specific genes related to the skin structure, repair mechanisms, sensitivity to environmental stressors, decreased cell turnover, impaired barrier function, and decreased expression of proteins, such as collagen and elastin, which play essential roles in maintaining skin elasticity and elasticity. Among the environmental factors, UVB and UVA cause degradation of the ECM components, such as hyaluronic acid and proteoglycan, damage to the cell structure due to chronic inflammation and oxidative stress, DNA damage, and promote collagen degradation. UVB irradiation causes oxidative stress in the cellular components, including lipids, proteins, and DNA. Their cumulative impact on the skin-aging process activates MMPs, contributing to collagen and elastin breakdown. This decreases the skin elasticity and causes wrinkle formation. In addition, UVB irradiation increases melanin synthesis [19-21]. The present study examined whether the IB complex could inhibit the skin damage caused by UVB-irradiated photoaging and oxidative stress through its effects on skin hydration, wrinkles, and melanogenesis.

HaCaT, Hs27, and B16F10 cells are the commonly used cell lines in skin health-related experiments. HaCaT cells are a human keratinocyte cell line that represents the epidermal cells of the skin. These cells are used widely to study the skin responses to external stimuli such as UV radiation or chemicals. Hs27 cells are a human fibroblast cell line representing the dermal cells of the skin. These cells are used to examine skin cell interactions and skin tissue regeneration. B16F10 cells are a mouse melanoma cell line used frequently in research on melanin production and skin whitening. These cells have a high melanin production capacity, making them a suitable model for evaluating skin whitening effects [22-24]. Each cell line represents different skin cell types, allowing researchers to study the skin physiology and pathology.

Maintaining optimal skin hydration is imperative for preserving the epidermal barrier function and overall skin health. This intricate process is orchestrated by the expression and regulation of various genes, each playing a crucial role in the intricate network governing skin hydration. Among these pivotal genes are collagen and elastin, which contribute to the structural integrity of the skin. In addition, HAS1-3 is involved in synthesizing hyaluronic acid, a key component in skin hydration. Furthermore, LCB1 and DEGS1 play essential roles in sphingolipid metabolism, helping to maintain the skin barrier. Sphingolipids are crucial components of the stratum corneum, the outermost layer of the epidermis, and are integral for preventing excessive water loss from the skin [25,26]. The degradation of the skin barrier is a multifaceted process influenced by various molecular factors. Among them, oxidative stress, nuclear factor kappa B (NF-κB), and COX-2 play crucial roles. Oxidative stress, characterized by an imbalance between ROS production and antioxidant defenses, contributes significantly to skin barrier dysfunction. The NF-κB, a transcription factor involved in inflammatory responses, has been implicated in regulating the genes associated

with immune and inflammatory reactions. Its activation is often observed in the context of skin barrier degradation, linking inflammation to the impairment of skin integrity [27-29]. These findings suggest that the IB complex mediates skin hydration by upregulating hyaluronic acid, sphingomyelin, collagen, *HAS 1-3*, *elastin*, *LCB1*, and *DEGS1*, and suppressing the NF-κB pathways and COX-2 in HaCaT cells.

The formation of skin wrinkles is intricately linked to the degradation of the ECM proteins, with MMP secretion and collagen fragmentation playing pivotal roles in this process. MMPs, a family of enzymes, are key players in ECM remodeling, and their increased activity is associated with the breakdown of structural components, particularly collagen. Collagen, a major protein in the ECM, provides the skin with strength and elasticity. The secretion of MMPs, such as MMP-1 (collagenase), MMP-2 (gelatinase), and MMP-3 (stromelysin), leads to the proteolytic cleavage of collagen fibers. This collagen fragmentation deteriorates the structural integrity of the skin, compromising its ability to resist deformation and maintain a smooth appearance [21,30,31]. The TGF-*β*/Smad pathway emerges as a pivotal regulatory mechanism governing collagen synthesis, playing a central role in maintaining skin homeostasis. In particular, previous studies have elucidated the intricate interplay between UV irradiation and the modulation of collagen metabolism. UV irradiation has a dual effect on the skin, orchestrating a complex molecular response. One facet of this response involves the up-regulation of MMPs through the mitogen-activated protein kinase (MAPK) pathway. MMPs, such as MMP-1, MMP-2, and MMP-9, are enzymes responsible for degrading various extracellular matrix components, including collagen. The activation of the MAPK pathway by UV irradiation helps increase the expression of MMPs, promoting the breakdown of collagen fibers. On the other hand, the TGF-*β*/Smad pathway, known for its role in collagen synthesis and fibrogenesis, is down-regulated in response to UV irradiation. This down-regulation of the TGF-*β*/Smad pathway contributes to a decrease in collagen expression, further exacerbating the imbalance in collagen homeostasis induced by UV exposure [32-34]. These results showed that the IB complex could protect against wrinkle formation by enhancing the *TGF-β*/Smad3 pathway and inhibiting the JNK/c-FOS/c-Jun/MMP pathway activation in Hs27 cells.

The induction of melanogenesis is closely associated with exposure to UV irradiation. Melanogenesis is the process by which melanocytes, specialized pigment-producing cells in the skin, synthesize and distribute melanin, the pigment responsible for skin color. UV irradiation, particularly in the form of UVB and UVA rays, is a potent stimulus for initiating and regulating melanin production. Upon exposure to UV radiation, melanocytes within the skin undergo a series of complex molecular responses. UVB radiation, in particular, directly activates melanocytes by triggering the DNA damage response, leading to the upregulation of various melanogenic enzymes, including tyrosinase. Tyrosinase is a key enzyme in the melanin synthesis pathway, catalyzing the conversion of tyrosine to melanin precursors, ultimately contributing to melanin production. In addition to direct effects on melanocytes, UV irradiation induces the release of signaling molecules, such as α-melanocyte-stimulating hormone (α-MSH), which further stimulates melanogenesis. This hormone binds to the melanocortin receptors on melanocytes, activating the cAMP signaling pathway and promoting the expression of melanogenic genes [35-37]. The present study indicated that the IB complex protected melanogenesis by glutathione synthesis, inhibiting tyrosinase activity and the cAMP/CREB/MITF pathway in B16F10 cells.

This study revealed the protective effects of the IB complex against UVB irradiation-induced skin dryness, oxidative stress, wrinkles, and melanogenesis in cellular models.

The IB complex uses a multifaceted approach to enhance skin health, promoting increased skin hydration by synthesizing hyaluronic acid and ceramide. Furthermore, it effectively inhibits wrinkle formation by modulating the JNK/c-FOS/c-Jun/MMPs pathway and reduces melanogenesis by down-regulating the PKA/CREB/MITF/TRP-1/TRP-2 pathway in response to UVB irradiation-induced oxidative stress. These findings suggest that supplementation with the IB complex holds significant promise as a preventive measure against skin photoaging. By targeting the key molecular pathways involved in skin hydration, wrinkle formation, and melanogenesis, the IB complex is a valuable candidate for maintaining skin health and combating the adverse effects of UVB irradiation on the skin.

REFERENCES

1. Coderch L, López O, de la Maza A, Parra JL. Ceramides and skin function. Am J Clin Dermatol 2003;4:107-29.
   PUBMED | CROSSREF

2. Tracy LE, Minasian RA, Caterson EJ. Extracellular matrix and dermal fibroblast function in the healing wound. Adv Wound Care (New Rochelle) 2016;5:119-36. PUBMED | CROSSREF

3. Chuong CM, Nickoloff BJ, Elias PM, Goldsmith LA, Macher E, Maderson PA, Sundberg JP, Tagami H, Plonka PM, Thestrup-Pederson K, et al. What is the 'true' function of skin? Exp Dermatol 2002;11:159-87.
   PUBMED | CROSSREF

4. Fisher GJ, Wang ZQ, Datta SC, Varani J, Kang S, Voorhees JJ. Pathophysiology of premature skin aging induced by ultraviolet light. N Engl J Med 1997;337:1419-28. PUBMED | CROSSREF

5. Rittié L, Fisher GJ. UV-light-induced signal cascades and skin aging. Ageing Res Rev 2002;1:705-20.
   PUBMED | CROSSREF

6. Dai G, Freudenberger T, Zipper P, Melchior A, Grether-Beck S, Rabausch B, de Groot J, Twarock S, Hanenberg H, Homey B, et al. Chronic ultraviolet B irradiation causes loss of hyaluronic acid from mouse dermis because of down-regulation of hyaluronic acid synthases. Am J Pathol 2007;171:1451-61. PUBMED | CROSSREF

7. Cavinato M, Jansen-Dürr P. Molecular mechanisms of UVB-induced senescence of dermal fibroblasts and its relevance for photoaging of the human skin. Exp Gerontol 2017;94:78-82. PUBMED | CROSSREF

8. Thilakchand KR, Mathai RT, Simon P, Ravi RT, Baliga-Rao MP, Baliga MS. Hepatoprotective properties of the Indian gooseberry (Emblica officinalis Gaertn): a review. Food Funct 2013;4:1431-41. PUBMED | CROSSREF

9. Kumar G, Madka V, Pathuri G, Ganta V, Rao CV. Molecular mechanisms of cancer prevention by gooseberry (Phyllanthus emblica). Nutr Cancer 2022;74:2291-302. PUBMED | CROSSREF

10. Akhtar MS, Ramzan A, Ali A, Ahmad M. Effect of Amla fruit (Emblica officinalis Gaertn.) on blood glucose and lipid profile of normal subjects and type 2 diabetic patients. Int J Food Sci Nutr 2011;62:609-16.
    PUBMED | CROSSREF

11. Tewari R, Kumar V, Sharma HK. Physical and chemical characteristics of different cultivars of Indian gooseberry (Emblica officinalis). J Food Sci Technol 2019;56:1641-8. PUBMED | CROSSREF

12. Kaur E, Bhardwaj RD, Kaur S, Grewal SK. Drought stress-induced changes in redox metabolism of barley (Hordeum vulgare L.). Biol Futur 2021;72:347-58. PUBMED | CROSSREF

13. Chełkowski J, Tyrka M, Sobkiewicz A. Resistance genes in barley (Hordeum vulgare L.) and their identification with molecular markers. J Appl Genet 2003;44:291-309. PUBMED

14. Kato E, Tsuruma A, Amishima A, Satoh H. Proteinous pancreatic lipase inhibitor is responsible for the antiobesity effect of young barley (Hordeum vulgare L.) leaf extract. Biosci Biotechnol Biochem 2021;85:1885-9. PUBMED | CROSSREF

15. Park SJ, Lee M, Oh DH, Kim JL, Park MR, Kim TG, Kim OK, Lee J. Emblica officinalis and Hordeum vulgare L. mixture regulates lipolytic activity in differentiated 3T3-L1 cells. J Med Food 2021;24:172-9. PUBMED | CROSSREF

16. Park SJ, Kim JL, Park MR, Lee JW, Kim OK, Lee J. Indian gooseberry and barley sprout mixture prevents obesity by regulating adipogenesis, lipogenesis, and lipolysis in C57BL/6J mice with high-fat diet-induced obesity. J Funct Foods 2022;90:104951. CROSSREF

17. Wünsch E, Heidrich HG. Zur quantitativen bestimmung der kollagenase. Hoppe Seylers Z Physiol Chem 1963;333:149-51.

18. Cannell RJ, Kellam SJ, Owsianka AM, Walker JM. Results of a large scale screen of microalgae for the production of protease inhibitors. Planta Med 1988;54:10-4. **PUBMED** | **CROSSREF**

19. Pillai S, Oresajo C, Hayward J. Ultraviolet radiation and skin aging: roles of reactive oxygen species, inflammation and protease activation, and strategies for prevention of inflammation-induced matrix degradation - a review. Int J Cosmet Sci 2005;27:17-34. **PUBMED** | **CROSSREF**

20. Chiang HM, Chen HC, Chiu HH, Chen CW, Wang SM, Wen KC. *Neonauclea reticulata* (Havil.) Merr stimulates skin regeneration after UVB exposure via ROS scavenging and modulation of the MAPK/MMPs/Collagen pathway. Evid Based Complement Alternat Med 2013;2013:324864. **PUBMED** | **CROSSREF**

21. Lan CE, Hung YT, Fang AH, Ching-Shuang W. Effects of irradiance on UVA-induced skin aging. J Dermatol Sci 2019;94:220-8. **PUBMED** | **CROSSREF**

22. Lee M, Kim D, Park SH, Jung J, Cho W, Yu AR, Lee J. Fish collagen peptide (Naticol®) protects the skin from dryness, wrinkle formation, and melanogenesis both *in vitro* and *in vivo*. Prev Nutr Food Sci 2022;27:423-35. **PUBMED** | **CROSSREF**

23. Kim MJ, Shin SY, Song NR, Kim S, Sun SO, Park KM. Bioassay-guided characterization, antioxidant, anti-melanogenic and anti-photoaging activities of *Pueraria thunbergiana* L. leaf extracts in human epidermal keratinocytes (HaCaT) cells. Processes. 2022;10:2156. **CROSSREF**

24. Lee B, Moon KM, Lee BS, Yang JH, Park KI, Cho WK, Ma JY. Swertiajaponin inhibits skin pigmentation by dual mechanisms to suppress tyrosinase. Oncotarget 2017;8:95530-41. **PUBMED** | **CROSSREF**

25. Wiest L, Kerscher M. Native hyaluronic acid in dermatology--results of an expert meeting. J Dtsch Dermatol Ges 2008;6:176-80. **PUBMED** | **CROSSREF**

26. Rabionet M, Gorgas K, Sandhoff R. Ceramide synthesis in the epidermis. Biochim Biophys Acta 2014;1841:422-34. **PUBMED** | **CROSSREF**

27. Sanchez J, Le Jan S, Muller C, François C, Renard Y, Durlach A, Bernard P, Reguiai Z, Antonicelli F. Matrix remodelling and MMP expression/activation are associated with hidradenitis suppurativa skin inflammation. Exp Dermatol 2019;28:593-600. **PUBMED** | **CROSSREF**

28. Chun KS, Langenbach R. A proposed COX-2 and PGE(2) receptor interaction in UV-exposed mouse skin. Mol Carcinog 2007;46:699-704. **PUBMED** | **CROSSREF**

29. Kondo S. The roles of cytokines in photoaging. J Dermatol Sci 2000;23 Suppl 1:S30-6. **PUBMED** | **CROSSREF**

30. Salminen A, Kaarniranta K, Kauppinen A. Photoaging: UV radiation-induced inflammation and immunosuppression accelerate the aging process in the skin. Inflamm Res 2022;71:817-31. **PUBMED** | **CROSSREF**

31. Lan CE, Hung YT, Fang AH, Ching-Shuang W. Effects of irradiance on UVA-induced skin aging. J Dermatol Sci 2019;94:220-8. **PUBMED** | **CROSSREF**

32. Tanaka Y, Uchi H, Ito T, Furue M. Indirubin-pregnane X receptor-JNK axis accelerates skin wound healing. Sci Rep 2019;9:18174. **PUBMED** | **CROSSREF**

33. Liarte S, Bernabé-García Á, Nicolás FJ. Role of TGF-β in skin chronic wounds: a keratinocyte perspective. Cells 2020;9:306. **PUBMED** | **CROSSREF**

34. Ke Y, Wang XJ. TGFβ signaling in photoaging and UV-induced skin cancer. J Invest Dermatol 2021;141:1104-10. **PUBMED** | **CROSSREF**

35. Park HY, Kosmadaki M, Yaar M, Gilchrest BA. Cellular mechanisms regulating human melanogenesis. Cell Mol Life Sci 2009;66:1493-506. **PUBMED** | **CROSSREF**

36. D'Mello SA, Finlay GJ, Baguley BC, Askarian-Amiri ME. Signaling pathways in melanogenesis. Int J Mol Sci 2016;17:1144. **PUBMED** | **CROSSREF**

37. Rzepka Z, Buszman E, Beberok A, Wrześniok D. From tyrosine to melanin: signaling pathways and factors regulating melanogenesis. Postepy Hig Med Dosw 2016;70:695-708. **PUBMED** | **CROSSREF**